https://doi.org/10.31436/iiumej.v25i1.2898

COMPACT CPW 4X4 MIMO ANTENNA FOR WI-FI 6 (IEEE802.11.AX) AND 5G(NR77/NR78/NR79) COMMUNICATIONS

NOORA SALIM[1*], MANDEEP J. SINGH[2] AND AMER T. ABED[3]

[1,2]Department of Electrical and Electronics Engineering,
Faculty of Engineering & Built Environment (FKAB)
Universiti Kebangsaan Malaysia, 43600 UKM Bangi, Selangor, Malaysia
[1]Faculty of Engineering, Al-Qasim Green University, Babylon, Iraq
[2]Space Science Center (ANGKASA), Institute of Climate Change,
Universiti Kebangsaan Malaysia, 43600 UKM Bangi, Selangor, Malaysia
[3]Department of Medical Instrumentation Techniques Engineering, Dijlah University College, Baghdad, Iraq

[*]Corresponding author: p110366@siswa.ukm.edu.my

(Received: 14 June 2023; Accepted: 12 July 2023; Published on-line: 1 January 2024)

ABSTRACT: This research proposes a compact 4x4 MIMO coplanar waveguide antenna for 5G NR and Wi-Fi 6 applications. The antenna has a size of 34x32x1.6 mm and operates in the 4.2-7 GHz band. By cutting slots on the ground and radiator, the mutual coupling is reduced to less than -15 dB between adjacent and opposite elements and less than -25 dB between diagonal elements. The antenna achieves good measured gains (3-6 dBi) and efficiency (60%-80%). The proposed antenna is suitable for high-performance wireless communication systems that require a small and low-cost MIMO antenna.

ABSTRAK: Kajian ini mencadangkan antena pandu gelombang yang kompak 4x4 MIMO koplanar bagi aplikasi 5G NR dan Wi-Fi6. Antena ini mempunyai saiz 34x32x1.6 mm dan beroperasi dalam kelompok gelombang 4.2-7 GHz. Dengan memotong slot pada tanah dan radiator, *mutual coupling* dikurangkan sebanyak -15 dB antara adjasen dan elemen bertentangan dan kurang daripada -25 dB antara elemen diagonal. Antena ini mencapai ukuran terbaik pada *gain* (3-6 dBi) dan kecekapan (60%-80%). Antena yang dicadangkan ini sesuai bagi sistem komunikasi tanpa wayar berprestasi tinggi yang memerlukan antena kecil dan murah seperti antena MIMO.

KEYWORDS: *slot; CPW; MIMO; Wi-Fi6; 5G*

1. INTRODUCTION

As new uses for the Internet of Things (IoT), smart cities, driverless vehicles, etc. have emerged, there has been a rise in the demand for fast wireless connections. Wi-Fi 6 (IEEE802.11ax) and 5G (nr77/nr78/nr79) are two examples of newly created standards that aim to address this need by delivering faster data speeds, lower latency, and more reliability. The requirements for wide bandwidth, high efficiency, high gain, and low mutual coupling that these standards impose provide new obstacles for antenna design. Furthermore, these standards operate at various frequency bands, making it challenging to create a universal antenna.

The literature reports a number of works on MIMO antenna design for 5G and Wi-Fi 6. However, most of these works suffer from some sort of restriction or flaw that prevents them from functioning at peak efficiency. Here, we evaluate several of these publications and discuss their merits and shortcomings.

In [1], one of the early works on MIMO antenna design for Wi-Fi 6 and 5G communications, a four-element CPW-fed MIMO antenna with a large impedance spectrum from 3 GHz to 11 GHz was proposed. To accomplish polarization diversity and great isolation, the design made use of four jug-shaped radiating devices with orthogonal polarization. The design's low gain, however, was consistent across the entire operating frequency range at -2 dB or less. The MIMO antenna studied in [2] was quite large and missed many critical frequencies, but its planar spiral line structure increased the diversity coefficient between dual radiating elements. In addition, [3] demonstrated a broad-bandwidth four-element CPW-fed MIMO antenna operating between 3 and 9 GHz, making it suitable for use in Wi-Fi 6 and 5G communications. To better isolate the two antenna parts, a rectangular slit was incorporated into the design, and a T-shaped stub was placed on the ground. The patch was designed with a U-shaped slot that produced a band notch at 5.5 GHz. Across the usable spectrum, this design's gain was just 0.5–2 dB, though.

For Wi-Fi 6 and 5G communications, an alternative MIMO antenna design was published in [3,4] which suggested a four-element MIMO antenna operating in three frequency bands: 0.5-1 GHz, 2.8-3.5 GHz, and 4.3-7.3 GHz. To achieve UWB performance, a rectangular patch was employed in conjunction with two inverted L-shaped slots and a rectangular slot. Band notches were also incorporated into the design by using two C-shaped slots at Wi-Fi and WLAN frequencies. However, this layout suffered from low efficiency at lower band and low gain at lower band in addition to its enormous 90x90x0.5 mm3 size.

In addition to the aforementioned works, others [5-9, 13-16] have reported on MIMO antenna design for Wi-Fi 6 and 5G communications. However, there are also downsides to these works that need to be considered. These include the works' bulkiness, bandwidth restriction, isolation coefficient, efficiency, gain, and missing frequencies. Table 2 provides a comparison of these previous works to the new design proposal.

Based on the reviewed literature, it is clear that a MIMO antenna design is needed that can operate over the frequency ranges needed for Wi-Fi 6 and 5G communications while still providing satisfactory results in terms of bandwidth, mutual coupling, efficiency, gain, and size. In this study, we present such a scheme and show how it improves upon prior proposals.

Using multiple-input multiple-output (MIMO) antennas, which improve wireless communication performance by spatial diversity and multiplexing, is one approach to this issue. MIMO antennas feature numerous radiating elements that may both send and receive data at the same time. However, creating MIMO antennas for Wi-Fi 6 and 5G communications is no easy task due to the need to strike a balance between multiple different aspects of their performance. For example: increasing the number of radiating elements can boost diversity gain and channel capacity, but it can also increase mutual coupling and lower efficiency. The antenna's bandwidth and gain can be compromised when its size is decreased to make it more portable.

Since Wi-Fi 6 and 5G communications both necessitate use of different frequency bands, this paper's primary objective is to offer a novel MIMO antenna design that can cover those spectrums while still providing respectable performance in terms of bandwidth, mutual coupling, efficiency, gain, and size. In order to increase isolation at high frequencies, the suggested design makes use of a coplanar waveguide (CPW) approach that employs four

https://doi.org/10.31436/iiumej.v25i1.2898

radiating components with orthogonal polarization and a floating parasitic element. The proposed design additionally employs a notch in the patch based on a split ring resonator (SRR) to block Wi-Fi and WLAN frequencies.

2. ANTENNA DESIGN AND ANALYSIS

2.1 Single Element Design

A CPW antenna was shown in Fig. 1a, where the ground and radiator were located on the same substrate face. On the ground plate, an elliptical slot E1 is cut with a major radius of mm and a minor radius of mm to form the antenna. The radiator fits into the elliptical slot E and has the following dimensions: W x L. The feeding strip line F with width (FW) and length (Fl) feeds the radiator. The feeding strip line F then becomes (f) with width (fw) and length (Fl) (fl). On the radiators S1 and S2, dual slots have been carved in order to produce greater resonant frequencies. Antenna dimensions Lg x Wg were etched with tan = 0.027, r = 4.3, and thickness = 1.6 mm on the FR-4 substrate. Table 2 shows all the planned antenna's dimensions as a single piece.

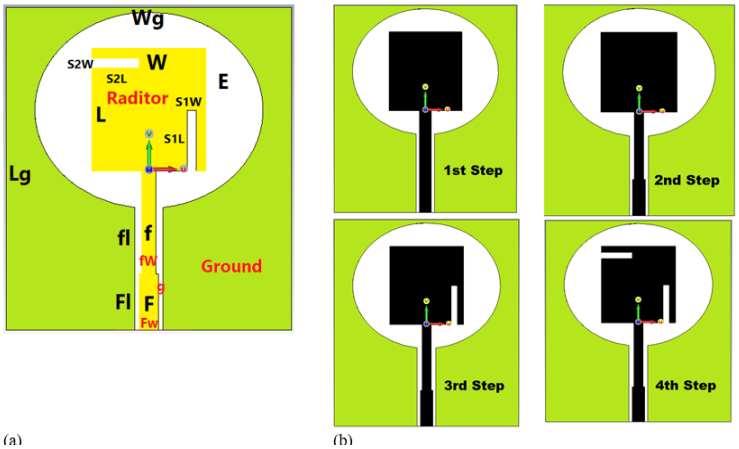

Fig. 1: Proposed antenna as a single element. (a) Single element, (b) Progress of antenna design.

It is clear that four procedures were necessary to create the recommended antenna as a single unit, as depicted in Fig. 1b. While the advancement of the impedance across the four design phases is shown in Fig. 2. The proposed antenna's working range at the first stage is shown by the dotted curve in Fig. 2 as being between 5 and 6.1 GHz. The width of the feeding line was altered at the second step to configure step impedance feeding the radiator, which resulted in the creation of more resonant frequencies that combined to produce a wide operating window of 4-5, 5 GHz, as shown in Fig. 2 (the dashed curve).

More resonant frequencies are produced when the radiator is divided by slot S1 r at the third stage of antenna construction. Thus, the dashed-dotted curve in Fig. 2 shows a large operating band of 4.1–6.1 GHz. As illustrated in the solid curve in Fig. 2, slot S2 added more frequencies to the antenna's impedance bandwidth, resulting in a wide band of 4.1–7 GHz that can handle a variety of wireless communications, including 5G (n78/n79) and Wi-Fi 6.

https://doi.org/10.31436/iiumej.v25i1.2898

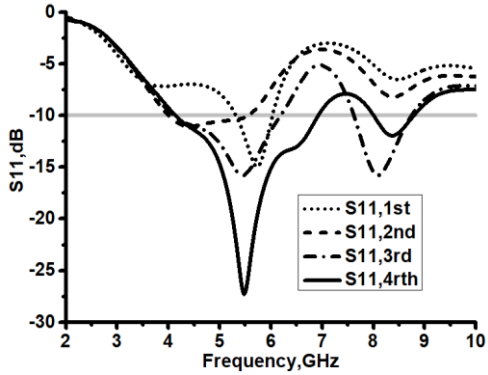

Fig. 2: The progress of the impedance of the antenna.

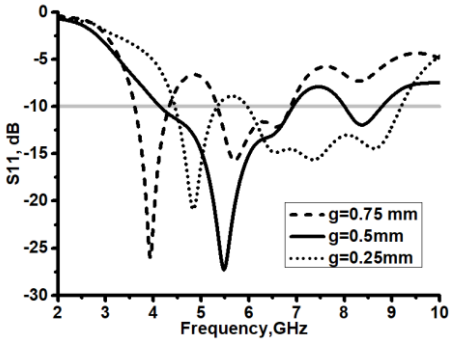

Fig. 3: The reflection coefficient with different gap.

The impact of altering the size of the gap g between the ground and the feeding line F on the antenna's impedance is depicted in Fig. 3. The antenna missed a crucial band for Wi-Fi 6 and 5G when g=0.75 mm when twin operational bands were observed (3.5-4.3 GHz and 5.4-6.2 GHz). The values of S11 were indicated by the dotted curve in Fig. 3. It is obvious that the antenna missed the most crucial region of 5-6 GHz when g=0.25 mm. Thus, as seen by the solid curve in Fig. 4, the gap's ideal size is 0.5 mm. The dimensions of the intended antenna as a whole are shown in Table 1.

Table 1: All dimensions of Spanner shaped antenna

Element	mm	Element	mm	Element	mm
$\mathbf{f_l}$	5.25	$\mathbf{S_{1w}}$	0.5	$\mathbf{L_g}$	16
$\mathbf{F_l}$	3	$\mathbf{S_{2w}}$	0.5	$\mathbf{W_g}$	15
$\mathbf{f_w}$	0.75	$\mathbf{S_{1l}}$	2.8	**W**	6
$\mathbf{F_w}$	1	$\mathbf{S_{2l}}$	2.5	**L**	6.5

2.2 MIMO Antenna Design

Figure 4 shows the structure of a MIMO antenna with four elements, the four elements etched on the FR-4 substrate with $\mathbf{W_w}$= 34 mm ,$\mathbf{L_l}$=32 mm and thickness of 1.6 mm. Despite the suggested 4x4 MIMO antenna's small size, the mutual coupling values between all radiating elements were so low that they indicated a significant degree of variety, as seen in Fig. 5. Antennas 1 and 2 and antennas 3 and 4 had mutual coupling values that ranged from -35 dB to -15 dB (see the dotted curve). According to the dashed curve in Fig. 5, the mutual coupling values between the adjacent antennas (antennas 1-3 and antennas 2-4) were less than -20 dB.

The mutual coupling between the crossed antennas (antennas 1-4 and antennas 2-3) was shown as a dashed-dotted curve, and it was discovered to be less than -30 dB during the operating range of 4.1 to 7 GHz.

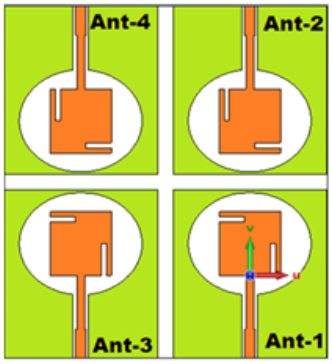

Fig. 4: 4x4 MIMO proposed antenna.

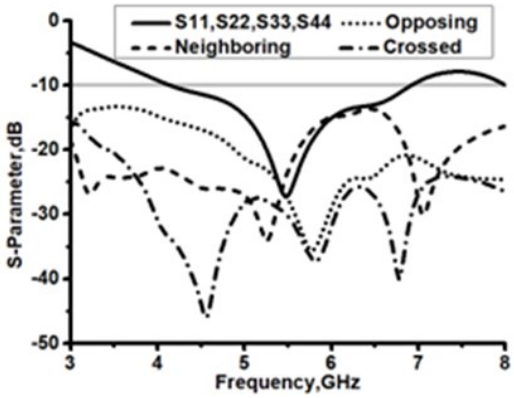

Fig. 5: Simulated mutual coupling between the radiating antennas.

3.3 Diversity Performance

The ECC can be calculated by either using three-dimensional (3D) radiation pattern values as in Eq. (1) or by using scattering parameter values as in Eq. (3) [8].

$$ECC_{ij} = \frac{\int_0^{2\pi}\int_0^{\pi} A_{ij}(\theta,\Phi)\sin\theta\, d\theta d\Phi}{\sqrt{\int_0^{2\pi}\int_0^{\pi} A_{ii}(\theta,\Phi)\sin\theta\, d\theta d\Phi \int_0^{2\pi}\int_0^{\pi} A_{jj}(\theta,\Phi)\sin\theta\, d\theta d\Phi}} \quad (1)$$

$$A_{ij} = XPR\,.E_{\theta,i}(\theta,\Phi)E^*_{\theta,j}(\theta,\Phi)P_{\theta}(\theta,\Phi) + E_{\Phi,i}(\theta,\Phi)E^*_{\Phi,j}(\theta,\Phi)P_{\Phi}(\theta,\Phi) \quad (2)$$

$$ECC_{ij} = \frac{|\, S^*_{ii}S_{ij}+S^*_{ji}S_{jj}\,|^2}{(1-|ii|^2-|S_{ji}|^2)(1-|S_{jj}|^2-|ij|^2)} \quad (3)$$

XPR means the cross-polarization ratio, $P_{\theta}(\theta,\Phi)$ $P_{\Phi}(\theta,\Phi)$ represent the incident power spectrum. ***In the MIMO system*** $E_{\theta,i}(\theta,\Phi)E^*_{\theta,j}(\theta,\Phi)$ and $E_{\Phi,i}(\theta,\Phi)E^*_{\Phi,j}(\theta,\Phi)$ represent the vertical (Θ) and horizontal (Φ) polarized radiation patterns of the antennas i and j,

https://doi.org/10.31436/iiumej.v25i1.2898

respectively. the vertical (Θ) and horizontal (Φ) polarized radiation patterns of the antennas i and j, respectively.

The envelope correlation coefficient (ECC) values between the opposite antennas (antennas 1- 2 and antennas 3 - 4) within the operating band of 4.1-7 GHz are less than 0.025 except in the working band of 4.1-7 GHz. The envelope correlation coefficient (ECC) values between the opposing antennas (antennas 1-2 and antennas 3-4) are less than 0.025, with the exception of the range of 4.1–4.2GHz, which reached 0.05 as indicated in the dotted curve in Fig. 6. Every ECC value between the adjacent antennas (antennas 1-3 and antennas 2-4) is less than 0.025 (the dashed black curve). The red dashed-dotted curve in Fig. 6 depicts ECC values that are less than 0.01 for all operational bands for crossed antennas (antennas 1-4 and antennas 2-3). As a result, by positioning the radiating components so that they matched the mutual coupling values shown in Fig. 5, the diversity between all radiating elements of the proposed MIMO antenna is increased.

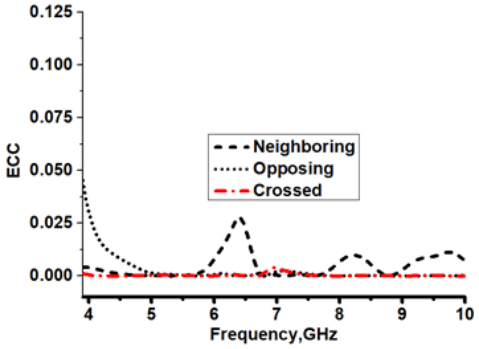

Fig. 6: Simulated ECC between opposite, neighboring, and crossed antennas.

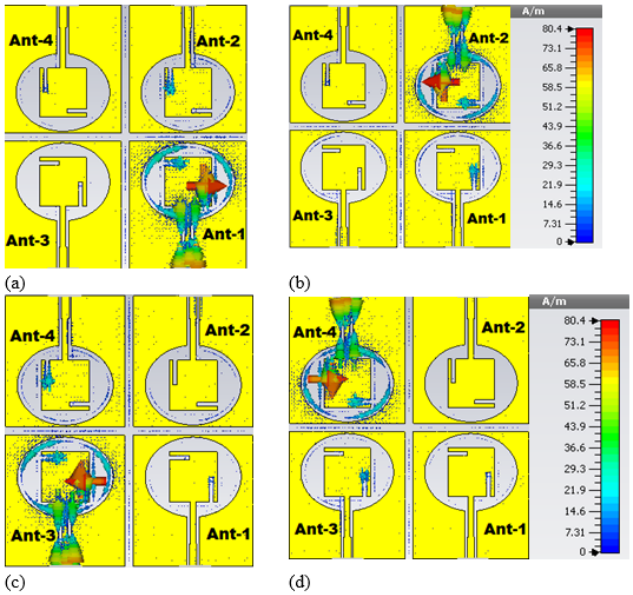

Fig. 7: The surface current distribution at resonant frequency 5.5 GHz for all elements.

2.4 Surface Current Distribution

For the surface current distribution at 5.5 GHz, the resonant frequency, is shown in Fig. 7. The current distribution is clearly seen to be largely dispersed along the feeding lines F, f, and the along the right side of the square radiator when antenna -1 is excited, as shown in Fig. 7a. For the resonant frequency of 5.5 GHz, the length of the surface current route is 22 mm, or

https://doi.org/10.31436/iiumej.v25i1.2898

almost half of a wavelength, which accounts for the low reflection coefficient S11 (-28 dB) result. Also, when antenna 1 is turned on, antenna 2 and 3 next to it show very little current distribution and little mutual coupling between the radiating elements, respectively. This suggests that the surface current is low. When antennas 2, 3, and 4 were activated, the same effect was observed (Fig. 7b, 7c and 7d). The analysis of the surface current distribution improved both the ECC values in Fig. 6 and the low mutual coupling value in Fig. 5.

3. MEASUREMENTS AND RESULTS

According to the prototype images in Fig. 8, the MIMO antenna's overall dimensions are 34 x 30 x1.6 mm. Figure 9 shows values for the simulated (solid curves) and measured (dashed-dotted curve) reflection coefficients of the MIMO antenna used in this study. The measured and simulated S-Parameters showed good agreement.

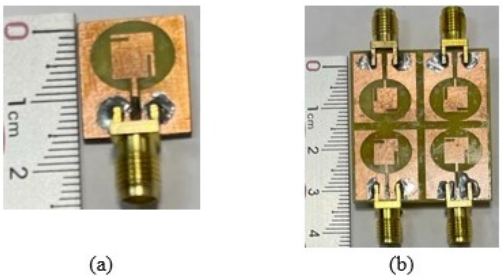

Fig. 8: Prototype photographs. (a) the single element, (b) the MIMO antenna.

For various wireless communications, including 5G (n77/n78/n790, Wi-Fi 6, and (Industrial, Scientific, and medical ISM), this operating band is advantageous. The measured impedance of the antenna (the black dashed-dotted curve) became 4.2-7 GHz. Within the working band, the mutual coupling values between the opposing antennas (antennas 1-2 and antennas 3-4) ranged from -15 dB to -25 dB (the red dashed-dotted curve). The mutual coupling values between the adjacent antennas (antennas 1-3 and antennas 2-4) ranged between -15 dB and -35 dB, according to the blue dashed-dotted curve in Fig. 9, while the mutual coupling values between the crossed antennas (antenna 1-4 and antennas 2-3) oscillated between -25 dB and -60 dB.

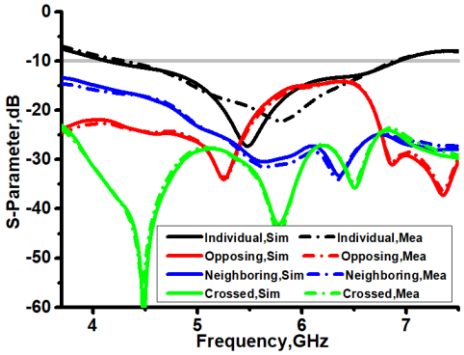

Fig. 9: The measured and simulated values of S-parameters.

By contrasting the SIR with and without the diversity scheme, the diversity gain can be determined. The diversity gain is defined as G = 10 log 10 (SIR d /SIR 0) (dB), where SIR d is the SIR with diversity and SIR 0 is the SIR without it [20],

https://doi.org/10.31436/iiumej.v25i1.2898

or

G (power factor) = SIR (d/0) (4)

Using numerous antennas at both ends of a MIMO communication link allows for a diversity strategy to be implemented. The channel matrix H, which represents the coefficients associated with each path between a send antenna and a receive antenna, is critical to the SIR with diversity. Without diversity, the SIR is a function of both the transmit antenna count (N t) and the receive antenna count (N r).

Using the channel matrix H's eigenvalues is one technique to get an approximation of the SIR while using diversity. Each spatial subchannel's effective gains in a MIMO system are represented by an eigenvalue. SNR is the signal-to-noise ratio, min(N t, N r) is the number of spatial subchannels, and min is the minimal eigenvalue of H, hence SIR d is a good approximation for the SIR with diversity.

Without diversity, you can use the average power of the channel matrix H to make an approximation of the SIR. The sum of all pathways' gains in a MIMO system is reflected in the average power. SIR 0 SNR ||H|| F 2 /N t where ||H|| F 2 is the Frobenius norm of H, equal to the sum of squares of all elements of H, and N t is the number of samples [20].

The formula for MIMO diversity gain can be derived using these approximations as follows:

The formula for generating G is as follows: G = 10 log 10 (SIR d /SIR 0) = 10 log 10 (SNR min(N t, N r) min /SNR 10 log 10 (min(N t, N r) min N t /||H|| F 2) = 10 log 10 (min(N t, N r)) + 10 log 10 (min) + 10 log 10 (N t) - 10 log 10 (||H|| F 2)

Power gain from spatial multiplexing is represented by the first term, and it grows as the number of spatial subchannels does. The second term, which represents the power boost from geographical variety, grows larger as the minimum eigenvalue of H decreases. As more transmit antennas are used, more power is lost, as represented by the third term, which is the result of transmit power split. The average power of H is shown in the fourth term, which indicates power loss due to channel fading.

We may use some statistical aspects of H to simplify this calculation if we assume that H contains independent and identically distributed (i.i.d.) entries with zero mean and unit variance. As an illustration, let's say that:

We can write E[||H|| F 2] = N t N r and E[min] = (1 -) /N r, where is Euler's constant.

Based on these assumptions, the typical MIMO diversity gain can be calculated as follows:

The formula for E[G] is as follows: -20 log 10 (e) + -20 log 10 ((1 -) /e + -20 log 10 (min(N t, N r) /N r) = -8.69 + 3.64 + 20 log 10 The ratio between the minimum and maximum values of N t and N r is 10.

The average MIMO diversity gain is calculated using this formula and is shown to depend exclusively on the ratio of min(N t, N r). Assuming that N t = N r = N leads to the following:

E[G] ≈ -5.05 dB (5)

The average diversity gain from using MIMO is less than 1, indicating that this type of system does not always improve diversity. This conclusion, however, relies on an average channel matrix H that may not accurately portray the channel state. The actual MIMO diversity gain could change depending on how H is realized and the signal-to-noise ratio (SNR) [20].

Figure 10 displays the proposed MIMO antenna's measured gain (the black circle dots) and efficiency (the blue square points). Gain for the proposed MIMO antenna varies between

https://doi.org/10.31436/iiumej.v25i1.2898

3dBi at 4 GHz and 6.dBi at 8 GHz. While the efficiency ratings ranged from 60% to 80%. Thus, during the working spectrum of 4.2-7 GHz, the recommended MIMO antenna had acceptable values of gain and efficiency.

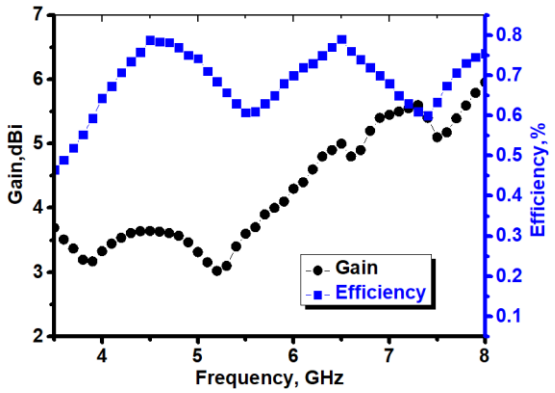

Fig. 10: Measured and simulated values of gain and efficiency for single and MIMO antenna.

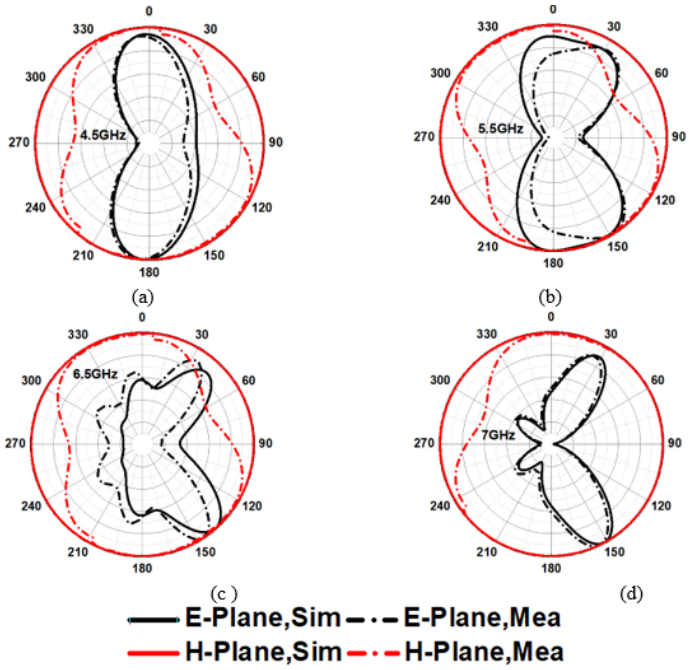

Fig. 11: Simulated and measured radiation patterns.

Displayed in Fig. 11 are the normalized radiation patterns at 4.5, 5.5, 6.5, and 7 GHz. There was a good degree of agreement between the measured patterns and the predicted patterns (the solid curves) (the dashed-dotted curves). All radiation patterns in the H-plane (4.5, 5.5, 6.5, and 7 GHz) are nearly omnidirectional. Figure 11a's black dashed-dotted curve, for example, lobes were identified at angles of 30° and 150° in the E-plane at 5.5 GHz, where the radiation pattern in that region became more directed (the black dashed-dotted curve, Fig. 11b). At the resonance frequency of 6.5 GHz, the black dashed-dotted curve in Fig. 11c displays twin major lobes at angles of 35° and 145° in the E-Plane as well as newly formed side lobes at angles of 350°, 300°, 235°, and 190°. The black dashed-dotted curve in Fig. 11d, at a frequency of 7 GHz, shows dual major lobes at angles of 30° and 150° and dual minor lobes at angles of 240° and 300°.

https://doi.org/10.31436/iiumej.v25i1.2898

Table 2 compares the proposed MIMO with other methods evaluated at [7,9, 11-16, 20-22, and 25]. All of the prior works listed in Table 3 were larger than this one, with the exception of [7,9,12, and 14]. The antennas used in the [12] experiment, however, only had a low isolation coefficient (9 dB), which does not support all necessary spectrum. Low isolation coefficients between radiating elements, low-efficiency values, missing the bands 5 GHz and 6 GHz for Wi-Fi 6, and missing the bands n78 and n79 for 5G all characterize the antenna described in [14]. Although having eight elements, the antennas reported in [22 and 25] had low efficiency and gain, especially at lower operating bands, and they failed to receive many of the necessary frequencies for Wi-Fi 6 and 5G.

Consequently, it is simple to state that the MIMO suggested in this study had a low profile, was compact, had minimal mutual coupling between radiation elements, acceptable values for gain, and covered the entire frequency range needed for Wi-Fi 6 and 5G communications.

Table 2: Comparison between proposed MIMO antenna and other related previous works

Ref.	No. El	B.W (GHz)	M. couple.	Effie. %	Gain (dB)	Size (mm^3)	Weakness
[1]	4	(1.95-2.5) (3.1-3.85) (4.95-6.6)	< -15	60-80	-1 to 2	40×40×1.6	Low values of gain
[2]	4	(3-9)	< -10	60-85	0.5-2	40×40×0.8	Low values of gain
[3]	4	(0.5-1) (2.8-3.5) (4.3-7.3)	< -10	10-90	-0.05-6.9	90×90×0.5	Large size, low efficiency at the lower band, low gain at the lower band
[4]	4	(3.26-3.88)	< -9	60-80	2-3.5	90×35×0.7	Large size, low isolation coefficient, does not support all required spectra
[5]	4	(4.23-4.82)	< -24	55-85	5-6	98×60×3	Large size, did not support 5G (n78, n79) and Wi-Fi 6
[6]	4	(3.4-4.3)	< -9	40-60	–	46×42×1.2	Did not cover all required band, no gain values reported, low efficiency, low isolation coefficient
[7]	4	(1.8-2.5)	< -10	51-73	-2.6 to 2.4	120×60×0.7	Large size, missed many required frequencies, low gain & efficiency at the lower band
[8]	4	(2.15-2.33)	< -11	75-85	–	100×60×0.8	Large size, narrow BW, there are no reports about values of gain and efficiency
[9]	4	(3.5 - 6)	< -10	40-80	–	150×57×7	Large size, missed many required frequencies, gain values not reported
[10]	4	(4.23-4.82)	< -24	55-85	5-6	98×60×3	Large size did not support 5G (n78,n79) and Wi-Fi 6
[11]	8	(3.3 - 5)	< -10	40-70	–	145×70×6	Large size, did not support 5G (n78/n79) and Wi-Fi 6, values of gain are not reported
[12]	8	(4.4 - 5)	< -22	20-55	-2.5 - 5	150×72×1	Large size did not support all required bands, low efficiency, low gain at the lower band
Proposed Design	4	(4.2 - 7)	< -15	60-80	3-6	34×32×1.6	

4. CONCLUSIONS

In this paper, we propose a novel MIMO antenna design that achieves high performance in terms of bandwidth, mutual coupling, efficiency, gain, and size while covering the frequency bands necessary for Wi-Fi 6 and 5G communications. In order to increase isolation at high frequencies, the proposed design makes use of a coplanar waveguide (CPW) technique that employs four radiating elements with orthogonal polarization and a floating parasitic element. To further avoid interfering with Wi-Fi and WLAN frequencies, the proposed design incorporates a notch in the patch that is based on a split ring resonator (SRR). The simulation and experimental results show that the proposed antenna has a wide bandwidth and good impedance matching in the frequency range of 4.2 GHz to 7 GHz. In addition to its high efficiency (from 60% to 80%) and high gain (from 3 dB to 6 dB) across the operating band, the proposed antenna also features high isolation (more than -15 dB) between its four radiating elements. In addition, the proposed antenna is smaller than most existing designs, coming in at just 34 x 32 x 1.6 mm^3. As a result, the proposed antenna is a viable option for both Wi-Fi 6 and 5G networks.

The proposed antenna's performance can be further enhanced by optimizing its design parameters in a future study. We also intend to put the proposed antenna through its paces in real-world scenarios, where its capabilities, diversity gain, and bit error rate will be put to the test. We intend to develop the proposed architecture further to incorporate support for additional wireless communication standards like LTE and WiMAX.

REFERENCES

[1] M. A. a. et.al. (2019) Mutual Coupling Suppression Between Two Closely Placed Microstrip Patches Using EM-Bandgap Metamaterial Fractal Loading. IEEE Access, 7: 23606 - 23614.

[2] O. A. S. Amjad Iqbal and A. B. a. A. B. (2018) Metamaterial-Based Highly Isolated MIMO Antenna for Portable Wireless Applications. MDPI, 7: 1-8.

[3] Y. C. Yan Pan, Chang Long Qi, RongLin Li. (2017) Evaluation of dual-polarised triple-band multibeam MIMO antennas for WLAN/WiMAX applications. IET Microwaves, Antennas & Propagation, 11: 1469-1475.

[4] J.-H. Xun, L.-F. S. , W.-R. L. , G.-X. L. , and S. C. (2017) Compact Dual-band Decoupling Structure for Improving Mutual Coupling of Closely Placed PIFAs. IEEE Antennas and Wireless Propagation Letters. 16: 1985 - 1989.

[5] Kumud Ranjan. et.al. (2021) 4-Port MIMO Antenna Using Common Radiator on a Flexible Substrate for Sub-1GHz, Sub-6GHz 5G NR, and Wi-Fi 6 Applications. IEEE Open Journal of Antennas and Propagation. 2: 689-701.

[6] Syed S. Jehangir and Mohammad S. Sharawi. (2020) A Compact Single Layer Four-Port Orthogonall Polarized Yagi-Like MIMO Antenna System. IEEE Transactions on Antennas and Propagation, 68: 1985 – 1989.

[7] Kin-Lu Wong et.al. (2020) Three Wideband Monopolar Patch Antennas in a Y-Shape Structure for 5G Multi-Input- Multi-Output Access Points. IEEE Antennas and Wireless Propagation Letters, 19: 393 - 397.

[8] Yu-Xuan Zhang. et.al. (2020) Low-Profile Wideband Conjoined Open-Slot Antennas Fed by Grounded Coplanar Waveguides for 4 × 4 5G MIMO Operation. IEEE Transactions on Antennas and Propagation, 68: 2646 - 2657.

[9] Hussain R, Sharawi MS. (2017) Annular slot-based miniaturized frequency-agile MIMO antenna system. IEEE Antennas and Wireless Propagation Letters, 16: 2489-2492.

[10] A. T. Abed. (2019) Fractal and Slot Antenna for Portable Communication Devices. Germany. LAP LAMBERT Acadmic Publication.

[11] A. T. Abed, et.al. (2021) Challenges and limits of fractal and slot antennas for WLAN, LTE, ISM, and 5G communication: a review paper. Annals of Telecommunications, 76(2): 547–557.

[12] Abed AT. (2020) A Novel Coplanar Antenna Butterfly Structure for Portable Communication Devices:A compact antenna with multioperating bands. IEEE Antennas and Propagation Magazine, 62(3): 83-89.
[13] A. T. Abed. (2019) Compact size MIMO amer fractal slot antenna for 3G, LTE (4G), WLAN, WiMAX, ISM and 5G communications. IEEE Access, 7: 125542-125551.
[14] A. T. Abed. (2020) Novel sunflower MIMO fractal antenna with low mutual coupling and dual wide operating bands. International Journal of Microwave and Wireless Technologies, 12(4): 323 – 331.
[15] Abed AT. (2018) Highly compact size serpentine-shaped multiple-input–multiple-output fractal antenna with CP diversity. Microwave, Antenna & Propagation, 12: 636-640.
[16] Ghalib A, Sharawi MS. (2017) TCM analysis of defected ground structures for MIMO antenna designs in mobile terminals. IEEE Access 5: 19680-19692.
[17] Park S-J, Myung-Hun J, Kyung-Bin B, Dong-Chan K, Laxmikant M. (2017) Performance comparison of 2 × 2 MIMO antenna arrays with different configurations and polarizations in reverberation chamber at millimetre-waveband Transactions on Antennas and Propagation 65: 6669-6678.
[18] Rajkumar S, Narayanaswamy VS, Sharada M and Krishnasamy TS. (2017) Heptaband swastik arm antenna for MIMO applications. IET Microwaves, Antennas & Propagation 11: 1255-1261.
[19] Saeed Khan M, Antonio DC, Adnan I, Raed MS and Dimitris EA. (2017) Ultra-compact dual-polarised UWB MIMO antenna with meandered feeding lines. IET Microwaves, Antennas and Propagation 11: 997-1002.
[20] Jin, Yuzhe. (2007) Capacity, Diversity and Multiplexing Gain for MIMO Channels. Microwaves 53: 667-676.